Variables Influencing Tumor Uptake of Anti-Melanoma Monoclonal Antibodies Radioiodinated Using Para-Iodobenzoyl (PIB) Conjugate

James L. Murray, Kalpana Mujoo, Christoph Wilmanns, Paul Mansfield, D. Scott Wilbur, and Michael G. Rosenblum

Departments of Clinical Immunology and Biological Therapy, Cell Biology and General Surgery, University of Texas M.D. Anderson Cancer Center, Houston, Texas and NeoRx Corporation, Seattle, Washington

Tumor uptake was examined with respect to antigen expression, time-dependent biodistribution, dose of Mab injected, tumor size, and tumor site (i.e., subcutaneous versus lung or liver metastases). NR-ML-05, 96.5, and P94 showed significantly greater uptake in subcutaneous tumors than CL207 and 5.1 ($p < 0.05$). NR-ML-05 had a significantly higher tumor uptake at 24 hr (11.9 ± 0.51) than at 72 hr (4.0 ± 0.37) or 144 hr (2.7 ± 0.84) after injection ($p < 0.001$). The other four Mabs had similar tumor distribution at all three time points. The tumor uptake of four Mabs (96.5, P94, CL207. 5.1) differed with respect to in vitro versus in vivo binding to tumor, tumor type, dose of Mab, and tumor site (subcutaneous versus metastases). In contrast, NR-ML-05 demonstrated consistent uptake in tumors independent of the above parameters. These data suggest that certain host parameters can influence in vivo tumor targeting depending on characteristics of each Mab studied.

J Nucl Med 1991; 32:279–287

The concept of delivering effective diagnostic and therapeutic doses of radionuclides coupled to monoclonal antibodies (Mabs) has been explored for more than 10 yr. Despite promising preclinical models and studies in man, these agents have had little impact in the clinical management of cancer patients. There are numerous possible reasons for this including variations in radiolabeling procedures (*1*), problems with antibody specificity and affinity (*2*), as well as other physical parameters which influence Mab uptake in tumors including tumor size (*3–5*), antigen content (*5*), blood flow (*6*), and Mab metabolism (*7–8*).

Received Apr. 11, 1990; revision accepted Aug. 2, 1990.

For reprints contact: James L. Murray, MD, Department of Clinical Immunology and Biological Therapy/Box 041, The University of Texas M.D. Anderson Cancer Center, 1515 Holcombe Blvd., Houston, TX 77030.

A significant problem regarding the use of iodine-labeled Mabs for diagnosis and therapy has been low tumor uptake and poor retention of radioiodine in tumors (i.e., <0.001% of injected dose/gram in many patient studies). This is believed to be due, in part, to dehalogenation of the antibody *in vivo* (*9*). To circumvent the in vivo deiodination, new methods of radioiodinating antibodies have been developed which employ radioiodinated small molecule conjugates (*10–13*) that do not have the ortho-iodophenol moiety (e.g., tyrosine) thought to be susceptible to enzymatic dehalogenation. Thus, rather than using the standard radioiodination method where direct coupling of radioiodine to the Mab's endogenous tyrosine residues occurs (*14, 15*), in this investigation radioiodination was carried out through the conjugation of N-succinimidyl para-iodobenzoate (PIB), a reagent that has been shown to be resistant to in vivo deiodination (*11*).

The PIB radioiodination procedure was used to compare the biodistribution of five anti-melanoma monoclonal antibodies, each recognizing a distinct antigen on melanoma cells. Xenografts derived from three individual melanoma cell lines were used for targets. Variables including tumor antigenicity, Mab immunoreactivity, time course of biodistribution, Mab dose, and tumor site (i.e., subcutaneous versus visceral metastases) were compared. We also examined whether in vitro binding of individual Mabs to the three different melanoma cell lines predicted in vivo localization in mice bearing subcutaneous tumors derived from these lines.

MATERIALS AND METHODS

Cell Lines

Characteristics of melanoma cell lines DX3, A375SM, and HS294t have been described previously (*16–18*). A375SM is a subclone of the parent line A375M (*17*). Cells were cultured in Eagles MEM (Cellgro Products, Houston, TX), supple-

mented with 10% fetal calf serum (Hyclone Products, Houston, TX) nonessential amino acids, 100 m*M* sodium pyruvate, 200 m*M* glutamine (Cellgro Products) and 0.05% gentamicin. They were routinely passaged once weekly and maintained at 37°C in a humidified incubator. All lines were free of mycoplasma contamination prior to use as determined using the Genprobe kit (Genprobe, Inc., San Diego, CA) for mycoplasma.

Monoclonal Antibodies

Murine anti-melanoma Mabs NR-ML-05, 96.5, P94, CL207, and 5.1 have been described previously (*19–23*) (Table 1). Mabs 96.5, P94, and 5.1 were supplied by Hybritech, Inc. (San Diego, CA) as ascites. These Mabs were purified using Protein A (Pharmacia, Uppsala, Sweden) or MAPS (Bio-Rad, Richmond, CA) affinity columns and then concentrated, using Amicon (Danvers, MA) filters, to a final concentration of ≥5 mg/ml in phosphate-buffered saline (PBS). Affinity purified Mab CL207 (IgG1) was a gift of Dr. Soldano Ferrone, Valhalla, NY. Purified NR-ML-05 was supplied by NeoRx Corporation in addition to two subclass-matched, irrelevant Mabs, NR-LU-10 (IgG2b) and NR2AD (IgG2a). NR-LU-10 binds to adenocarcinomas whereas NR2AD reacts with the idiotype of a B-cell lymphoma cell line. Mab 15A8, an IgG1 murine Mab reactive with breast carcinoma, was supplied by Dr. Renato Dulbecco, LaJolla, CA. This Mab served as the subclass-matched control Mab for both CL207 and 5.1. Screening of Mab binding prior to labeling was performed using ELISA technique (*24*). The binding of all the antibodies to each of the three cell lines was found to be two- to five-fold greater than the control Mabs.

Antibody Labeling Using PIB

The standard para-iodobenzoyl (PIB) labeling procedure for low levels of iodine-125 (^{125}I) or ^{131}I has been described previously (*11*). This method conjugates N-succinimidyl-para-iodobenzoate to the Mab. Briefly, 37.5 μl of a mixture of 1% HOAc/MeOH, 10 μl of a 1 mg/ml MeOH solution of N-chlorosuccinimide (NCS) and 10 μL PBS were sequentially added to a reaction vial (fitted with a septum) containing N-succinimidyl 4-tri-μ-butylstannylbenzoate ($12.5\ \mu g, 2.5 \times 10^{-2}$ μmole) in 12.5 μl 1% HOAc/MeOH. One millicurie of either ^{125}I (melanoma-specific Mabs) or ^{131}I (control Mabs) was added to the reaction solution and after 5 min the reaction was quenched by the addition of $NaHSO_3$ ($10\ \mu l, 7.5 \times 10^{-2}$ μmole. The MeOH solvent was evaporated under N_2 gas for 10 minutes. 500 μg of Mab in 100 μl PBS was mixed with 100 μl borate buffer (pH 9.3) and then added to the reaction vial. Conjugation was allowed to proceed for 5 min at room temperature. Radiolabeled Mab was separated from unreacted radioiodine by chromatography on sephadex G-25 (PD-10) (Pharmacia) columns. Radiochemical yield ranged from 40% to 60%; incorporation of radiolabel into Mabs measured by TCA precipitation was greater than 90%. The specific activity of radiolabeled Mabs ranged between 0.2 and 0.3 μCi/μg. The immunoreactivity and affinity of each Mab was evaluated using the Lindmo method (*25*) (Table 1).

Live Cell Radioimmunoassay

Binding of radiolabeled murine Mab to melanoma cells was examined using a previously published RIA technique (*26*). Cells were harvested from subconfluent cultures using trypsin-EDTA (0.01% trypsin in 0.02% EDTA), washed twice in complete medium, and seeded in flat-bottomed microtiter plates at a concentration of 0.5 to 1×10^4 cells/well. Following a 24-hr incubation at 37°C, 5% CO_2, growth medium was aspirated and 100 μl of 10% bovine serum albumin (BSA) (wt/vol) in MEM (Cellgro Products) medium containing 0.8% sodium azide was added to each well. After a 1-hr incubation at 37°C, the medium was gently aspirated and cells were washed once with BSA-containing medium. One hundred microliters of radiolabeled Mabs (concentration: 1.5 to 10 μg/ml in MEM containing 1% BSA) was added to each well for 60 min. Following an additional 60-min incubation at 37°C, cells were washed four times with MEM containing 1% BSA and 100 μl of 1% Nonidet NP-40 (Sigma Chemical Corp., St. Louis, MO) was added to lyse cells. The fluid in each well was absorbed onto a cotton swab and radioactivity was measured in a gamma counter (Packard Instruments, Des Plaines, IL). Background counts per minute (wells containing media alone) were subtracted from experimental wells. All binding experiments were done in triplicate. The amount of antibody bound was expressed as the mean counts per minute per 10^5 cells.

Athymic Mouse Studies

Six-week-old athymic (nude) mice were obtained from Simonsen Laboratories (Gilroy, CA). Mice were maintained in specific pathogen-free conditions and were used at 8–10 wk

TABLE 1
Antibody Characteristics

Melanoma Mab	Subclass	Antigen	Immunoreactivity (i.e., after labeling)	Affinity constant
NR-ML-05	IgG2b	240Kd Proteoglycan	70%	6.6×10^9 M-1
96.5	IgG2a	97Kd Glycoprotein	50%	3.3×10^9 M-1
P94	IgG2a	94Kd Glycoprotein	70%	8×10^{10} M-1
CL207	IgG1	96Kd Glycoprotein	55%	3.14×10^8 M-1
5.1	IgG1	210Kd Protein	N.T.*	N.T.

* N.T. = not tested.

of age. Subcutaneous and visceral xenografts were established as follows:

Subcutaneous Model: DX3, A375SM and HS294t melanoma cells were harvested while in log phase from plastic T150 tissue culture flasks using 0.01% Trypsin, 0.02% EDTA solution. Cells were counted, washed and suspended in Hanks balanced salt solution (HBSS) (Gibco, Grand Island, NY). Viability was greater than 90%. The cell suspension was adjusted to a concentration of 1×10^7 cells/ml and 0.1 ml of suspension was injected into the subcutaneous tissue overlaying the right chest wall near the anterior axillary line of each mouse. At 4–5 wk when tumors had reached 0.5–2 cm in size, 5 μg of each ^{125}I-labeled melanoma-specific Mab was injected i.v. simultaneously with 5 μg of the respective ^{131}I-labeled control Mab. Mice were killed at various times (24, 72, and 144 hr) following injection. Tumor and normal heart, lung, spleen, liver, kidney, stomach and intestine, and muscle were removed, weighed, rinsed in normal saline to remove blood contamination, and assayed for radioactivity on a gamma counter with windows set for dual-channel counting of ^{125}I and ^{131}I. The percentage of injected Mab/g (%ID/g) in tumor and normal organs was calculated as:

$$\frac{^{125}\text{I}/^{131}\text{I cpm/g tissue}}{^{125}\text{I}/^{131}\text{I injected (corrected for decay)}} \times 100.$$

Tumor-to-blood (T:B) or tumor-to-organ ratios were calculated by dividing the %ID/g Mab in tumor by the %ID/g Mab in the respective organ. The specificity of localization (localization index = LI) for each melanoma Mab relative to its subclass-matched control Mab was calculated as:

$$\frac{\%\text{ID specific Mab in tumor} \div \%\text{ID specific Mab in blood}}{\%\text{ID control Mab in tumor} \div \%\text{ID control Mab in blood}}.$$

Localization indices greater than one denote specific localization.

Metastatic Models: Methods for establishing liver metastases as well as lung metastases from intrasplenic or i.v. injections of melanoma cells have been described previously (*27*). Liver metastases were generated by injection of 0.5×10^6 DX3 melanoma cells into the splenic capsule using a 30-gauge needle. At 6–8 wk, animals demonstrated abdominal distension and at autopsy had macroscopic tumor nodules in the liver. Similarly, lung metastases were generated by i.v. injection of 1×10^6 A375SM melanoma cells. Gross metastatic nodules appeared in the lungs of mice at eight weeks following injection. Following injection of 5 μg of each of the respective Mabs, tumors were dissected free from surrounding normal tissue. T:B ratios, %ID/g Mab in tumor in tissues, and LIs were calculated as above. In all cases, there was no microscopic tumor present in normal liver, however it was difficult to separate gross tumors in lung from surrounding normal lung. From 5–10 mice/group were used per experiment. In some cases, additional mice were used (up to 20 per group) to confirm previous observations.

Statistical Analysis

One-way analysis of variance (ANOVA) and Students' t-test for independent means was used to determine significance between groups. Results were expressed as mean ± standard error of the mean (s.e.m.).

RESULTS

Mab Specificity and Kinetics of Localization In Vivo

Each of the five Mabs were radiolabeled with ^{125}I and injected simultaneously along with the subclass-matched ^{131}I-labeled control Mab into groups of mice bearing A375SM subcutaneous xenografts. At either 24, 72, or 144 hr after injection, mice were killed and the %ID/g in tumor, blood, and visceral organs was determined. T:B ratios were determined for each Mab and the LIs were calculated as described. The mean ± s.e.m. %ID/g uptake for each Mab in tumor at the respective time points along with LIs at each time point are shown in Table 2. Of the five Mabs, NR-ML-05, 96.5, and P94 demonstrated greater localization in terms of %ID/g compared to either CL207 or 5.1 at 24 or 72 hr postinjection ($p < 0.05$). With the exception of Mab NR-ML-05, there was no statistically significant difference in tumor localization at 24, 72, or 144 hr for Mabs 96.5, P94, CL207, and 5.1. NR-ML-05 demonstrated three-fold greater uptake in tumor at 24 hr compared to 72 hr and 144 hr ($p < 0.001$). Significantly higher localization indices were observed at 144 hr for NR-ML-05 and at 72 hr for 96.5 and P94 compared to other time points ($p < 0.05$). These data reflect a higher T:B ratio for specific versus nonspecific Mab at these times. In view of the lack of significant differences in %ID/g between time points in four of the five antibodies tested, as well as the higher LIs at 72 hr for two of the Mabs, subsequent experiments were performed 72 hr after Mab injection.

Except for NR-ML-05 where the T:B ratio at 144 hr (2.7 ± 0.43) was significantly higher than at 24 hr (0.70 ± 0.11, $p < 0.001$), there were no significant differences in T:B ratios at 24, 72, or 144 hr for the remaining Mabs (Table 2). A comparison of T:B and tumor:organ ratios for NR-ML-05 localization versus NR-LU-10 (control) localization in mice with A375SM tumors is shown in Figure 1. Significantly higher ratios were observed for specific compared to nonspecific Mabs. For NR-ML-05, the highest ratios observed were tumor-to-liver (10.2 ± 1.2) and tumor-to-stomach and intestine (23.5 ± 3.6).

In Vitro Versus In Vivo Mab Immunoreactivity

Table 3 compares the in vitro binding of each of the melanoma-specific Mabs to each of the three cell lines with in vivo uptake at 72 hr in the respective subcutaneous xenografts. In vitro binding of each Mab to each cell line varied significantly. Similar differences were noted in vivo; moreover, there was not a positive correlation between in vitro binding and targeting of Mabs to the respective tumor grown in vivo. For example, for cell line DX3, the degree of immunoreactivity between

TABLE 2
Kinetics of Mab Localization in A375SM Tumors

Mab	%ID/g (LI)* 24 hr	T:B ratio	72 hr	T:B ratio	144 hr	T:B ratio
NRML	11.9§ ± 0.51 (2.5)	0.70 ± 0.11	4.0 ± 0.37 (5.3)	1.9 ± 0.28	2.7 ± 0.84 (8.2)‡	2.7¶ ± 0.43
96.5	5.1 ± 0.97 (1.7)	0.60 ± 0.09	4.8 ± 0.78 (3.1)‡	1.7 ± 0.55	2.6 ± 0.18 (1.9)	0.60 ± 0.11
P94	3.6 ± 0.99 (2.3)	0.87 ± 0.37	3.3 ± 0.39 (6.8)‡	1.4 ± 0.27	2.3 ± 0.47 (N.T.)†	1.2 ± 0.24
CL207	N.T.	—	2.3 ± 0.33 (2.2)	0.92 ± 0.08	1.6 ± 0.24 (1.6)	0.86 ± 0.12
5.1	2.2 ± 0.30 (1.3)	0.54 ± 0.09	2.2 ± 0.44 (1.1)	0.52 ± 0.04	1.9 ± 0.25 (N.T.)	0.45 ± 0.06

* L.I. = localized index (see Materials and Methods). Values represent mean of 10 mice per group
† N.T. = not tested.
‡ LI significantly increased versus 24 and 72 hr (NRML-05; $p < 0.05$), OR vs. 24 and 144 hr (96.5 and P94; $p < 0.05$).
§ Significantly greater ($p < 0.001$) compared to 72 and 144 hr.
¶ Significantly greater ($p < 0.001$) compared to 24 hr.

each of the five Mabs (expressed as cpm/10^5 cells) was as follows: NR-ML-05 >96.5 >P94 >CL207 >5.1, respectively ($p < 0.001$). In contrast, the %ID/g in DX3 tumors was significantly greater for CL207 (6.5 ± 0.85) compared to each of the other Mabs ($p < 0.001$). Antibody 96.5 had very poor localization in DX3 tumors (0.94 ± 0.20) despite excellent in vitro binding. In spite of its low in vivo uptake, it was still specific for the tumor compared to its control Mab (LI = 1.5 ± 0.11). For cell line A375SM, the degree of Mab reactivity in descending order was: NR-ML-05 >P94 >96.5 >CL207 >5.1 ($p < 0.001$), whereas in vivo targeting of Mabs was equivalent for NR-ML-05, P94, and 96.5 (4.0 ± 0.37, 4.8 ± 0.78, and 3.3 ± 0.39, respectively; $p > 0.05$). For HS294t, binding of NR-ML-05 and P94 was significantly greater ($p < 0.001$) than binding of each of the other three Mabs, a pattern which was also observed in vivo. Of the three most reactive Mabs, NR-ML-05, P94, and 96.5, only NR-ML-05 had identical localization to all three subcutaneous xenografts.

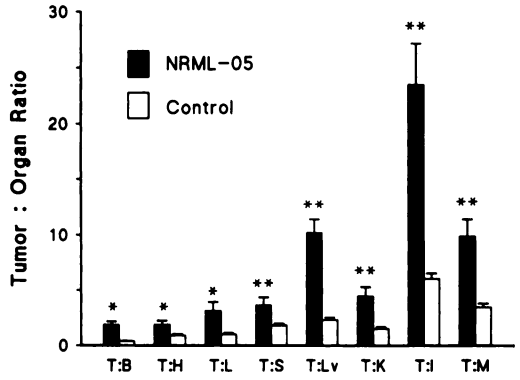

FIGURE 1
Tumor-to-blood (T:B) and tumor:organ (T:O) ratios of NR-ML-05 versus its subclass-matched control Mab NR-LU-10. Key: T:H = tumor:heart; T:L = tumor:lung; T:S = tumor:spleen; T:LV = tumor:liver; T:K = tumor:kidney; T:I = tumor:stomach and intestines; and T:M = tumor:muscle. Significantly higher ratios (*$p < 0.025$; **$p < 0.001$) were noted for NR-ML-05 compared to control. n = 10 mice/group.

Since tumor size has been shown to influence Mab targeting in previous studies (*3–5*), with smaller tumors having a greater percentage of Mab uptake/g than larger tumors, we compared uptake of individual Mabs in tumors with respect to mean tumor size (Table 3). Although there was a significant variation in mean ± s.e.m. size of tumors among the three different cell lines, there was not a statistically significant inverse correlation between mean %ID/g Mab in tumor and this parameter ($p > 0.05$, ANOVA). This finding was also observed in mice bearing both large (1.34 ± 0.24) and small (0.11 ± 0.03) subcutaneous A375SM tumors who received ^{125}I-labeled NR-ML-05 (large = 3.1 ± 0.58 %ID/g; small = 3.4 ± 0.32 %ID/g, $p > 0.05$).

Effect of Mab Dose on Tumor Uptake

While the binding of 96.5 to DX3 cells in vitro was among the highest tested, the uptake of 96.5 by DX3 xenografts in vivo was among the lowest of the group tested. To determine whether this finding was related to dose of the Mab administered, 1 μg of each ^{125}I-labeled Mab was admixed with increasing concentrations of unlabeled Mab and injected into mice bearing DX3 tumors. As shown in Table 4, increasing concentrations of unlabeled Mabs had no effect on any of the five radiolabeled Mabs' localization in tumors, except for P94 where the %ID/g tumor for 5 μg Mab (i.e., 1 μg labeled plus four unlabeled) or 101 μg Mab (1 μg labeled plus 100 μg unlabeled) was significantly greater than that found for 1 μg labeled Mab ($p < 0.001$).

Additional studies in mice bearing DX3 xenografts demonstrated that NR-ML-05 had a slightly greater localization in DX3 tumors at 24 hr (5.7 ± 1.9%ID/g) compared to 72 hr (2.5 ± 0.26%ID/g; $p < 0.01$), similar to what was observed for A375SM xenografts. To study whether the interval between injections of unlabeled versus labeled antibody, as well as time of localization

TABLE 3
Comparison of In Vitro Binding to In Vivo Localization of Mabs at 72 Hours

Mab	A375SM	Tumor size	DX3	Tumor size	HS294T	Tumor size
			In Vitro			
NR-ML-05	3682 ± 417*	—	4287 ± 139	—	1879 ± 262	—
96.5	929 ± 47	—	2914 ± 204	—	1005 ± 60	—
P94	2464 ± 247	—	2195 ± 239	—	2413 ± 199	—
CL207	505 ± 59	—	335 ± 165	—	526 ± 217	—
5.1	22†	—	412	—	1025	—
			In Vivo			
	4.0 ± 0.37‡	0.97 ± 0.09§	2.5 ± 0.26	2.1 ± 0.21	3.4 ± 0.64	0.20 ± 0.06
	4.8 ± 0.78	0.59 ± 0.16	0.94 ± 0.20	1.01 ± 0.25	1.7 ± 0.32	0.27 ± 0.06
	3.3 ± 0.39	1.42 ± 0.25	2.0 ± 0.27	1.5 ± 0.20	4.6 ± 0.59	0.37 ± 0.06
	2.3 ± 0.33	0.65 ± 0.11	6.5 ± 0.85	1.2 ± 0.21	2.2 ± 0.37	0.39 ± 0.05
	2.2 ± 0.12	1.19 ± 0.09	2.6 ± 0.32	1.3 ± 0.28	2.8 ± 0.54	0.21 ± 0.05

* Data expressed as mean ± s.e.m. cpm/10^5 cells for three experiments.
† Mean of duplicate experiments.
‡ Data expressed as mean ± s.e.m. %ID/g (5–10 mice/group).
§ Mean ± s.e.m. tumor size in grams for each group.
There was significant variation in size between the different tumors (A375SM vs. DX3 vs. HS294t = $p < 0.001$, ANOVA).

(24 versus 72 hr) could influence tumor uptake, 4, 100, 250, or 500 μg of unlabeled NR-ML-05 was injected into mice-bearing DX3 tumors 1 hr prior to injection of 1 μg ^{125}I-labeled NR-ML-05. As shown in Figure 2, targeting of ^{125}I-labeled was not affected following preinjection of up to 250 μg unlabeled Mab. At 500 μg, however, there was a 50% decrease in %ID/g (1.4 ± 0.09) compared to the other dose levels ($p < 0.001$; ANOVA), indicating specific blocking of radiolabeled Mab uptake by unlabeled Mab.

Localization in Subcutaneous Versus Visceral Metastases

Table 5 compares tumor uptake of four Mabs in subcutaneous tumors of both DX3 and A375SM cell lines with tumor uptake in lung (A375SM) and liver metastases (DX3). The most significant findings were that the %ID/g uptake of 96.5 and 5.1 in lung tumors was significantly greater than their respective localization in subcutaneous tumors. In contrast, 96.5, P94, and 5.1 localized to a significantly lesser extent in liver metastases compared to subcutaneous tumors. NR-ML-05 localized in subcutaneous and visceral tumors to a similar degree. Although the increased %ID/g of 96.5 and 5.1 in lung tumors versus subcutaneous tumors correlated inversely with tumor size ($p < 0.01$), there was not a similar correlation between localization of the other Mabs and tumor size. There was no significant difference ($p > 0.05$) in the T:B ratios for each anti-melanoma Mab between subcutaneous and visceral metastases with the exception of Mab 5.1 (Table 5). Moreover, there was no significant difference in localization of subclass-matched control Mabs between subcutaneous and visceral sites with the exception of 15A8 (A375SM subcutaneous = 1.9 ± 0.15; A375SM lung = 2.8 ± 0.65; DX3 subcutaneous = 2.5 ± 0.60; DX3 liver = 6.9 ± 0.07; $p < 0.005$). Localization indices for each Mab were greater than one in all instances (range 1.1 for Mab 5.1 to 4.4 for Mab NR-ML-05). Except for Mab 5.1 (subcutaneous = 1.2 ± 0.07; liver = 1.7 ± 0.14; $p < 0.05$), LIs did not vary significantly between subcutaneous and metastatic models.

DISCUSSION

This study is a systematic evaluation of several host parameters influencing Mab uptake in tumors using a series of anti-melanoma Mabs labeled with I-125 by the para-iodobenzoyl conjugate technique (*11*). The most significant findings from this study were:

1. Mab reactivity varied significantly with respect to in vitro versus in vivo binding, tumor type, and

TABLE 4
Effect of Mab Mass on Tumor Localization (DX3) at 72 Hours

Mab	Mab Dose μg*	5 μg	100 μg
96.5	0.48 ± 0.19†	0.52 ± 0.16	0.75 ± 0.04
P94	0.44 ± 0.16	2.2 ± 0.59‡	2.1 ± 0.28‡
CL207	4.2 ± 0.97	6.5 ± 0.86	5.9 ± 0.43
5.1	2.2 ± 0.74	2.5 ± 0.49	1.6 ± 0.09

* In each case 1 μg of ^{125}I-labeled Mab was administered alone or admixed with 4 or 99 μg of unlabeled Mab.
† Values reflect mean ± s.e.m. %ID/g. n = 5 mice/group.
‡ %ID/g significantly greater for 5 μg and 100 μg Mab.

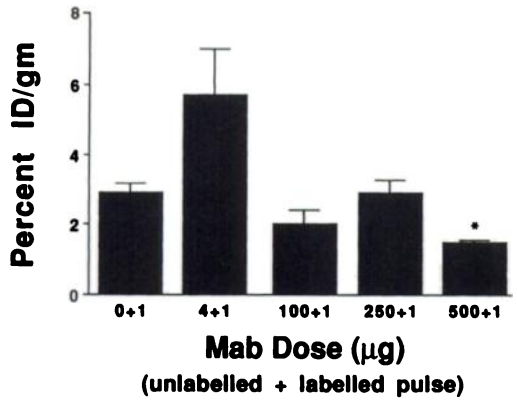

FIGURE 2
Tumor uptake of NR-ML-05 in subcutaneous xenografts of DX3 at 24 hr. Mice were given escalating doses of unlabeled NR-ML-05 (from 0 to 500 μg) followed 1 hr later by 1 μg ^{125}I-labeled NR-ML-05. A significant decrease (*$p < 0.001$) in tumor uptake of labeled NR-ML-05 occurred following injection of 500 μg unlabeled Mab compared to the other four groups. n = 5 mice/group.

tumor site (i.e., subcutaneous tumors versus metastases)

2. Except for Mab P94, injection of increasing doses of unlabeled Mab did not significantly enhance tumor uptake of labeled Mab.
3. In contrast to the other Mabs, NR-ML-05 targeting was unaffected by the above parameters (tumor type, tumor site, or in vitro versus in vivo binding).

Tumor uptake of four Mabs (96.5, P94, CL207, and 5.1) did not seem to vary greatly with respect to time studied after injection. NR-ML-05, on the other hand, had a greater tumor uptake at 24 hr. This finding was consistent for both A375SM and DX3 xenografts, which argues against differences in antigen expression between cell lines as being a significant factor. The T:B ratios for all five Mabs were not significantly different at each time point, except for NR-ML-05 which had a T:B ratio of 0.70 ± 0.11 at 24 hr compared to 2.7 ± 0.43 at 144 hr ($p < 0.001$). Collectively, these data suggest that Mab binding and clearance were occurring in the tumor at similar rates. A drop in uptake of NR-ML-05 between 24 and 72 hr could be the result of a faster metabolism and clearance of this Mab (*7*). Previous studies using Mabs labeled with ^{125}I by the iodogen or chloramine-T method have demonstrated considerable dehalogenation in the first 24 hr, resulting in an increase in T:B ratios secondary to a rapid disappearance of radionuclide from blood (*28*). The constant blood levels of radioactivity as well as the high ratios of Mab in tumor with respect to stomach and intestines (Fig. 1) indicate that iodination of Mabs by the PIB method results in a more stable conjugate (*11*). These data differ significantly from studies using indium-111 (^{111}In) as the radionuclide in which uptake of conjugates in liver has resulted in tumor-to-liver ratios of 1.0 or less due to sequestration and metabolism of ^{111}In-conjugate (*29,30*). Furthermore, our observed results for intact antibodies labeled by the paraiodobenzoyl con-

TABLE 5
Variability in Tumor Uptake: Subcutaneous (s.c.) Versus Liver or Lung Metastases

	A375SM			
Mab	s.c.	Tumor size (g)	Lung	Tumor¶ size (g)
NR-ML-05	3.3 ± 0.52 (1.7)*	0.97 ± 0.09	4.6 ± 0.40 (1.3)	0.17 ± 0.02
96.5	2.8 ± 0.22 (1.8)	0.60 ± 0.16	8.4† ± 2.2 (1.3)	0.17 ± 0.03
P94	3.3 ± 0.39 (1.4)	1.4 ± 0.25	3.6 ± 1.3 (1.7)	0.36 ± 0.10
5.1	2.0 ± 0.28 (0.34)	1.2 ± 0.09	4.34† ± 0.49 (0.28)	0.23 ± 0.04
	DX3			
	s.c.	Tumor size (g)	Liver	Tumor¨ size (g)
	2.5 ± 0.28 (1.6)	2.1 ± 0.21	3.2 ± 0.86 (2.2)	1.5 ± 0.24
	1.2 ± 0.28 (0.47)	1.9 ± 0.25	0.53‡ ± 0.09 (0.51)	1.0 ± 0.27
	2.0 ± 0.26 (0.47)	1.5 ± 0.20	0.55§ ± 0.09 (0.23)	0.74 ± 0.27
	2.5 ± 0.49 (0.58)	1.3 ± 0.28	0.49§ ± 0.06 (0.33)‡	0.61 ± 0.12

* Numbers in parentheses represent T:B ratios for each model. n = 10 mice/group.
† Significantly greater than s.c. model ($p < 0.01$).
‡ Significantly less than s.c. model ($p < 0.05$).
§ Significantly less than s.c. model ($p < 0.01$).
¶ Lung tumors significantly smaller than s.c. tumors; $p < 0.005$.
¨ Liver tumors smaller than s.c. tumors; $p = 0.05$.

jugate method had considerably lower T:B ratios (range 0.54–2.7) from those previously reported when the similar meta-iodobenzoyl conjugate method (*31*) was used (T:B = 10:1) or ^{111}In-Mabs conjugated using the mixed anhydride technique were used (*30,32*). However, caution must be used when comparing results from separate studies in which antibodies against different tumor types and having differing affinities and immunoreactivities were used. Indeed, valid comparisons are likely to only be obtained in dual isotope administrations in animals (or patients) to eliminate the host of variables presented in differing studies.

A previous study using ^{111}In-labeled Mabs 96.5 and ZME018, a Mab recognizing a different epitope of the HMW melanoma antigen, has shown that binding of the above Mabs to each of the three cell lines was not predictive of in vivo localization (*32*). This has been confirmed in studies using other Mabs in which this variability was due either to alternation of cell lines in culture (*33*) or modulation of in vivo antigenicity (*32*). Hence, the data presented confirms the above results and suggests that differential in vitro reactivity and in vivo tumor uptake do not appear to be dependent on the isotope used to label Mabs.

Preclinical (*34*) as well as clinical trials (*35,36*) using ^{111}In-labeled Mabs have demonstrated that the addition of increasing amounts of unlabeled Mabs prior to or concomitant with a small amount of radiolabeled Mab caused an increase in Mab targeting to tumor. Other human trials have not demonstrated this effect (*37,38*). In this study, increasing the amount of unlabeled Mab up to 100 μg had little effect on tumor uptake of the respective radiolabeled Mabs, except for P94 which demonstrated improved tumor localization following injection of 5 μg Mab and above. These data suggest that saturable clearance mechanisms might be dependent on physical characteristics of each Mab used and/or the antigen which it recognizes. Mab-recognizing antigens that are shed into the circulation (such as CEA) have been shown to demonstrate this effect due to immune complex formation and targeting to liver (*39*). Whether the method of labeling, antigen expression, or isotope used plays a significant role in this phenomenon is unclear, although preliminary data examining ^{111}In-labeled 96.5 targeting to HS294t subcutaneous tumors has shown tumor uptake to be dependent on dose (*40*). In this study, in vivo data derived from injecting increasing amounts of unlabeled NR-ML-05 followed by labeled NR-ML-05 demonstrated that the total antigen pool was quite high since saturation occurred at a Mab dose between 250 and 500 μg.

A unique finding of this study was that tumor uptake in subcutaneous xenografts differed from that in lung and liver metastases for four of the five Mabs studied. Previous studies by Fidler (*27*) have shown that the biologic behavior of human tumors in nude mice is influenced by their site of implantation and growth and our study corroborates this. Other variables affecting Mab localization include growth rate (*41*), vascularity (*6*), and physical parameters, including the rate of Mab diffusion into tissues (*42*) and Mab metabolism (*8*). Although the mechanism(s) underlying our findings are unknown, it is unlikely that differences in Mab metabolism, or vascular permeability, played a significant role because the T:B ratios did not differ between the subcutaneous and visceral models. This is in contrast to previous studies using ^{111}In-labeled Mab 96.5 in which T:B ratios were significantly different between subcutaneous xenografts and liver metastases (*8*). The reason(s) for these findings most likely is due to differences in liver metabolism of ^{125}I-PIB labeled Mabs versus ^{111}In-labeled Mabs (*43*). Whether site-dependent antigen modulation can account for differences in uptake between subcutaneous and metastatic tumors is an important issue (*32*). Additional experiments are being designed to measure antigen expression of tumors in different tissues.

NR-ML-05 showed the least variability among the five Mabs tested with respect to in vivo binding to the three cell lines, Mab dose, tumor site, or tumor size. Studies in man have demonstrated that the 240 KD high MW antigen is more homogeneously distributed than other anti-melanoma Mabs when measured in separate biopsies between patients as well as multiple biopsies in the same individual (*44*). This parameter may account for the favorable biodistribution and superior tumor imaging using Fab fragments of this Mab (*45*) or a similar Mab recognizing the identical antigen in man (*46*). The effect on tumor size on Mab uptake depends on antigen expression (*5*), degree of tumor necrosis (*4*), or method of Mab labeling (*5*). Our data are compatible with those of others using ^{125}I-PIB-labeled Mab NR-ML-05 (Wilbur DS, unpublished data), but differ from those of Hagan et al. (*4*) using ^{111}In-labeled antimelanoma Mabs. Part of the discrepancy between our study and others may relate to the method of data analyses. For example, if tumor size in an individual animal was correlated with the %ID/g in tumor, a significant ($p < 0.05$) inverse correlation was observed between 5.1 and CL207 with cell line A375SM, NR-ML-05 and CL207 with DX3, and NR-ML-05, 96.5 and CL207 with HS294t (data not shown). Hence, corresponding with another report (*5*), the influence of tumor size varied depending on the Mab and cell line used.

In conclusion, the biodistribution of labeled anti-melanoma Mabs in human tumors grown in athymic mice varied depending on tumor type, Mab dose, and tumor site. Similar findings have been noted in clinical trials (*46,47*). Hence, these data may serve as an indication of the complex mechanisms of Mab-based imaging and therapy.

ACKNOWLEDGMENTS

The authors wish to acknowledge and thank: Dr. Soldano Ferrone for generously donating Mab CL207; Hybritech, Incorporated for supplying Mabs 96.5, 5.1 and P94; Dr. Charles Morgan for supplying Mabs NR-ML-05, NR2AD, and NR-LU-10, and Dr. Dulbecco for donating Mab 15A8. We also wish to thank Dr. Stephen Hadley, Dr. Mark Hylarides, and Peggy Janus for technical assistance and Carolyn Wheat for manuscript preparation.

This work was supported by Public Health Service Grant CA43544 awarded by the National Cancer Institute.

REFERENCES

1. Bhargava KK, Acharya SA. Labeling of monoclonal antibodies with radionuclides. *Semin Nucl Med* 1989;19:187–201.
2. Halpern SE, Dillman RO. Problems associated with radioimmunodetection and possibilities for future solutions. *J Biol Resp Modif* 1987;6:235–262.
3. Philben VJ, Jakowatz JG, Beatty BG, et al. The effect of tumor CEA content and tumor size on tissue uptake of indium-111-labeled anti-CEA monoclonal antibody. *Cancer* 1986;57:571–576.
4. Hagan PL, Halpern SE, Dillman RO, et al. Tumor size: effect on monoclonal antibody uptake in tumor models. *J Nucl Med* 1986;27:422–427.
5. Watanabe Y, Endo K, Koizumi M, et al. Effect of tumor mass and antigenic nature on the biodistribution of labeled monoclonal antibodies in mice. *Cancer Res* 1989;49:2884–2889.
6. Sands H, Jones PL, Shah SA, et al. Correlation of vascular permeability and blood flow with monoclonal antibody uptake by human Clouser and renal cell xenografts. *Cancer Res* 1988;48:188–193.
7. Pimm MV, Baldwin RW. Comparative biodistribution and rates of catabolism of radiolabeled anti-CEA monoclonal antibody and control immunoglobulin in nude mice with human tumour xenografts showing specific antibody localization. *Eur J Nucl Med* 1987;3:258–263.
8. McCready DR, Price J, Balch CM, et al. Altered biodistribution of indium-111-labeled monoclonal antibody 96.5 to tumors and normal tissues of nude mice bearing human melanoma xenografts in visceral organs. *Cancer Immunol Immunother* 1989;30:257–261.
9. Carrasquillo JA. Radioimmunoscintigraphy with polyclonal or monoclonal antibodies. In: Zalutsky MR, ed. *Antibodies in radiodiagnosis and therapy.* Boca Raton, FL: Raven Press, 1988:169–198.
10. Zalutsky MR, Narula AS. Radiohalogenation of a monoclonal antibody using an N-succinimidyl-3-(tri-n-butylstannyl)-benzoate intermediate. *Cancer Res* 1988;48:1446–1450.
11. Wilbur DS, Hadley SW, Hylarides MD, et al. Development of a stable radioiodinating reagent to label monoclonal antibodies for radiotherapy of cancer. *J Nucl Med* 1989;30:216–226.
12. Hadley SW, Wilbur DS. Evaluation of iodovinyl antibody conjugates:comparison with a p-Iodobenzoyl conjugate and direct radioiodination. *Bioconj Chem* 1990;1:154–161.
13. Srivastava PC, Allred JF, Buchsbaum DJ. Radioiodinated iodophenyl maleimide: A potential radioimmunoconjugate with low in vivo deiodination. *Nuc Compact-Eur/Amer Commun in Nucl Med* 1990;5:145–149.
14. Fischer PJ, Speck JC. Protein and cell membrane iodinations with a sparingly soluble chloramide 1, 3, 4, 6-tetrachloro-3α-6α-diphenylglycouril. *Biochem Biophys Res Commun* 1978; 80:849–857.
15. Osterman LA. Labeling of the proteins. in: *Methods of protein and nucleic acid research.* New York: Springer-Verlag; 1984:131–133.
16. Albino AP, Lloyd KO, Houghton AN. Heterogeneity in surface antigen and glycoprotein expression of cell lines derived from different melanoma metastases of the same patient. *J Exp Med* 191;154:1764–1778.
17. Kozlowski JM, Hart IR, Fidler IJ, et al. A human melanoma line heterogeneous with respect to metastatic capacity in athymic nude mice. *JNCI* 1984;72:913–917.
18. Creasey AA, Smith JS, Hackett AJ, et al. Biological properties of human melanoma cells in culture. *In Vitro* 1979;15:342–350.
19. Morgan AC, Galloway DR, Reisfeld RA. Production and characterization of monoclonal antibody to a melanoma specific glycoprotein. *Hybridoma* 1981;1:27–36.
20. Brown JP, Nishiyama K, Hellstrom I, Hellstrom KE. Structural characterization of human melanoma associated antigen P97 with monoclonal antibodies. *J Immunol* 1981;127:539–546.
21. Imai K, Wilson BS, Bigotti A, Natali PG, Ferrone S. A 94,000-dalton glycoprotein expressed by human melanoma and carcinoma cells. *JNCI* 1982;68:761–769.
22. Matsui M, Temponi M, Ferrone S. Characterization of a monoclonal antibody-defined human melanoma-associated antigen susceptible to induction by immune interferon. *J Immunol* 1987;139:2088–2092.
23. Loop SM, Nishiyama K, Hellstrom I, et al. Two human tumor-associated antigens, P155 and P210, detected by monoclonal antibodies. *Int J Cancer* 1981;27:775–781.
24. Mujoo K, Cheresh DA, Yang HM, Reisfield RA. Disialoganglioside GD2 on human neuroblastoma cells:target antigen for monoclonal antibody-mediated cytolysis and suppression of tumor growth. *Cancer Res* 1987;47:1098–1104.
25. Lindmo T, Boven E, Cuttita F, Fedorko J, Bunn Jr PA. Determination of the immunoreactive fraction of radiolabeled monoclonal antibodies by linear extrapolation to binding at infinite antigen excess. *J Immunol Methods* 1984; 72:77–89.
26. Greiner JW, Hand PH, Noguchi P, et al. Enhanced expression of tumor-associated antigens on human breast and colon tumor cells after recombinant human leukocyte α-interferon treatment. *Cancer Res* 1984;44:3208–3214.
27. Fidler IJ. Rationale and methods for the use of nude mice to study the biology and therapy of human cancer metastases. *Cancer Met Rev* 1986;5:29–49.
28. Hayes DF, Zalutsky MR, Kaplan W, et al. Pharmacokinetics of radiolabeled monoclonal antibody B6.2 in patients with metastatic breast cancer. *Cancer Res* 1986;46:3157–3163.
29. Bernhard MI, Hwang KM, Foon JM, et al. Localization of ^{111}In and ^{125}I-labeled monoclonal antibody in guinea pigs bearing line 10 hepatocarcinoma tumors. *Cancer Res* 1983;43:4429–4433.
30. Halpern SE, Hagen PL, Garver PR, et al. Stability characterization and kinetics of ^{111}In-labeled monoclonal antibodies in normal animals and nude mouse-human tumor models. *Cancer Res* 1983;43:5347–5355.
31. Zalutsky MR, Noska MA, Colapinto EV, Garg PK, Bigner DD. Enhanced tumor localization and in vivo stability of a monoclonal antibody radioiodinated using N-succinimidyl 3-(tri-n-butylstannyl)-benzoate. *Cancer Res* 1989;49:5543–5549.
32. McCready DR, Balch CM, Fidler IJ, Murray JL. Lack of comparability between binding of monoclonal antibodies to melanoma cells in vitro and localization in vivo. *JNCI* 1989;81:682–687.
33. Real FX, Fliegel B, Houghton AM. Surface antigens of human

melanoma cells cultured in serum-free medium: induction of expression of major histo-compatibility complex class II antigens. *Cancer Res* 1988;48:686–693.
34. Otsuka FA, Welch MJ. Evidence for a saturable clearance mechanism for ^{111}In-labeled monoclonal antibodies. *Intl J Nucl Med Biol* 1985;12:331–332.
35. Murray JL, Lamki LM, Shanken LJ, et al. Immunospecific saturable clearance mechanisms for indium-111-labeled anti-melanoma monoclonal antibody 96.5 in humans. *Cancer Res* 1988;48:4417–4422.
36. Carrasquillo JA, Abrams PG, Schroff RW, et al. Effect of antibody dose on the imaging and biodistribution of indium-111 9.2.27 anti-melanoma monoclonal antibody. *J Nucl Med* 1988;29:39–47.
37. Wahl RL, Wilson BS, Liebert M, et al. High-dose, unlabeled, nonspecific antibody pretreatment: influence on specific antibody localization to human melanoma xenografts. *Cancer Immunol Immunother* 1987;24:221–224.
38. Halpern SE, Haindl W, Beauregard J, et al. Scintigraphy with In-111-labeled monoclonal antitumor antibodies: kinetics, biodistribution and tumor detection. *Radiology* 1988;168: 529–536.
39. Beatty BG, Beatty JD, Williams LE, et al. Effect of specific antibody pretreatment on liver uptake of ^{111}In-labeled anti-carcinoembryonic antigen monoclonal antibody in nude mice bearing human colon cancer xenografts. *Cancer Res* 1989;49:1587–1594.
40. McCready DR, Murray JL, Balch CM, et al. Coadministration of un-labeled monoclonal antibody (Mab) enhances tumor uptake and decreases non-tumor uptake of ^{111}In-labeled 96.5 in nude mice. *Proc AACR* 1988;29:426.
41. Rostock RA, Klein JL, Kopher KA, et al. Variables affecting the tumor localization of ^{131}I-antiferritin in experimental hepatoma. *Am J Clin Oncol* 1984;7:9–18.
42. Jain RK. Transport of molecules in the tumor interstitium: a review. *Cancer Res* 1987;47:3039–3051.
43. Jones PL, Brown BA, Sands H. Uptake and metabolism of ^{111}In-labeled monoclonal antibody B6.2 by the rat liver. *Cancer Res* 1990;50(suppl):8523–8565.
44. Natali P, Bigotti A, Cavaliere R, et al. Heterogeneous expression of melanoma associated antigens and HLA antigens by primary and multiple metastatic lesions removed from patients with melanoma. *Cancer Res* 1985;45:2883–2889.
45. Salk D. Technetium-labeled monoclonal antibodies for imaging metastatic melanoma: results of a multi-center clinical study. *Semin Oncol* 1988;15:608–618.
46. Murray JL, Rosenblum MG, Lamki L, et al. Clinical parameters related to optimal tumor localization of indium-111-labeled mouse antimelanoma monoclonal antibody ZME-018. *J Nucl Med* 1987;28:25–33.
47. Epenetos AA, Snook D, Durbin H, et al. Limitations of radiolabeled antibodies for localization of human neoplasms. *Cancer Res* 1986;46:3183–3191.

EDITORIAL

Biologic Characterization of Melanoma Tumors by Antigen-Specific Targeting of Radiolabeled Anti-Tumor Antibodies

Over the past decade, considerable progress has been made in the use of anti-tumor monoclonal antibodies for targeting human tumors in vivo, both for the purpose of diagnosis (*1*) and for therapy, particularly of radiosensitive tumors such as lymphoma (*2*, *3*). In a brief summary of the clinical aspects of this work, it can be stated that "proof of principle" has been achieved: namely, that otherwise clinically occult tumors are detectable by these methods (*4*, *5*) and that durable remissions in chemotherapy-resistant human tumors (lymphomas) (*6*) and neuroblastoma (*7*) have been produced. The use of Technetium-99m-labeled antibodies promises to make diagnostic applications more and more practical in the future (*8*). The increasing availability of stem cell stimulating factors and autologous marrow rescue procedures promises to be effective in reducing marrow toxicity, which is the critical organ for current radioimmunotherapy regimens (*9*).

Thus, the reader is probably already familiar with the use of monoclonal antibodies (Mabs) for the purpose of diagnosis and therapy of human tumors. I would like to use this occasion to discuss an additional in-vivo use for radiolabeled antibodies; namely, to characterize, based on external imaging of radioactivity uptake, the biologic features of tumors in terms of the expression of specific antigens as markers for known stages of cell differentiation, or as structural components related to specific functions of the tumor cell.

In this issue of *The Journal of Nuclear Medicine* (*10*), Murray et al. focus upon a component of the multi-factorial problem of the mechanisms of radiolabeled antibody targeting to human xenograft tumors in animal models by focusing on "host-factors," which may alter uptake. The principal finding of the paper is that tumor site can influence in vivo tumor uptake, in a manner that is dependent on the antibody used. Four out of the five antibodies used, showed altered uptake when melanoma tumors were in the lung or liver site, in comparison to subcutaneous sites.

It is clear that certain biologic features of tumors and characteristics of currently available anti-tumor antibodies may limit the amount of uptake of the radiolabeled monoclonal antibodies (*11–31*). Table 1 summarizes factors that are known to influence the uptake of radiolabeled antibodies into human tumor xenografts in animal models. Some of these have been confirmed in human tumors.

A review of Table 1 should convince even the most casual reader that the localization of radiolabeled monoclonal antibodies to human cancers is a complicated process that is influenced by diverse biologic and technical features. Improved understanding is important, however,

Received Dec. 11, 1990; accepted Dec. 11, 1990.
For reprints contact: Steve Larson, MD, Nuclear Medicine Dept., Memorial Sloan Kettering Cancer Center, NYC, NY.